High contrast dark resonances in a cold-atom clock probed with counterpropagating circularly polarized beams

X. Liu, V. I. Yudin, A. V. Taichenachev, J. Kitching, and E. A. Donley

Citation: Appl. Phys. Lett. **111**, 224102 (2017);
View online: https://doi.org/10.1063/1.5001179
View Table of Contents: http://aip.scitation.org/toc/apl/111/22
Published by the American Institute of Physics

High contrast dark resonances in a cold-atom clock probed with counterpropagating circularly polarized beams

X. Liu,[1] V. I. Yudin,[2,3,4] A. V. Taichenachev,[2,3] J. Kitching,[1] and E. A. Donley[1,a)]
[1]National Institute of Standards and Technology, 325 Broadway, Boulder, Colorado 80305, USA
[2]Novosibirsk State University, Novosibirsk 630090, Russia
[3]Institute of Laser Physics, Siberian Branch of Russian Academy of Sciences, Novosibirsk 630090, Russia
[4]Novosibirsk State Technical University, Novosibirsk 630092, Russia

(Received 22 August 2017; accepted 12 November 2017; published online 29 November 2017)

A cold-atom coherent population trapping clock based on $\sigma_+ - \sigma_-$ interrogation realized by counter-propagating optical fields of opposite circular polarization is presented. The simultaneous use of σ_+ and σ_- polarizations prevents atoms from being trapped in the end magnetic sublevels, significantly enhancing the contrast over interrogation with a single circular polarization. Because the system is based on cold atoms and there is very little relaxation, nearly complete dark states are created, and coherent population trapping resonances with maximum contrast are observed. A frequency stability of $1.3 \times 10^{-11}/\sqrt{\tau}$ is achieved, which averages down to 2×10^{-13} after a 40 000 s integration period. https://doi.org/10.1063/1.5001179

Compact high-performance microwave atomic clocks are applied widely in many fields, including telecommunications and navigation systems. In an atomic clock based on coherent population trapping (CPT),[1–4] the microwave interrogation that probes the atoms is optically carried, eliminating the need for a microwave cavity. Thus, CPT atomic clocks are smaller and use less power, which enabled the development of chip-scale atomic clocks.[5–7] Vapor-cell CPT clocks have demonstrated outstanding short-term stability,[8–12] but their long-term frequency stability critical for many potential applications has been limited by frequency shifts from high-pressure buffer gases and light shifts.[7,8,11,12] The shift and associated instability from buffer gases can be eliminated by performing CPT with cold atoms.[13–15] Using laser-cooled atoms also eliminates Doppler broadening, thus narrowing the atoms' optical spectra and creating a clean system where all cold atoms are uniformly interrogated and light shifts can be precisely studied.[16] CPT clocks based on cold atoms may find use in commercial applications needing improved long-term stability if miniaturization techniques for laser cooling are successful.[17–20]

Traditional CPT clocks interrogate atoms with bichromatic light of a single circular polarization to create Λ systems that connect magnetic sublevels in each hyperfine ground state through a common excited state. When the difference between the two optical frequencies exactly equals the hyperfine ground-state splitting, the atoms can be optically pumped into a dark state and stop absorbing light. But interrogation with a single circular polarization also traps atoms in the extreme Zeeman magnetic sublevels with the highest angular momentum, m_F, where they do not contribute to the dark resonance. This results in CPT resonance signals with relatively low amplitude.

To overcome the loss from trap states and maximize the CPT resonance amplitude, several optimized interrogation schemes have been demonstrated, including push-pull optical pumping (PPOP),[21] $\sigma_+ - \sigma_-$,[22] lin$\perp$lin,[23] and lin $\parallel$ lin.[24] The PPOP, $\sigma_+ - \sigma_-$, and lin $\perp$ lin schemes all interrogate the $m_F = 0 \rightarrow m_F = 0$ hyperfine clock transition via the double-Λ scheme shown in Fig. 1(a) by applying a combination of σ_+ and σ_- polarizations to the atoms with various approaches. Unique from the other three schemes, the lin $\parallel$ lin technique[24] interrogates a double-Λ system with $\Delta m_F = 2$ transitions between the $m_F = \pm 1$ levels in the ground states and will not be discussed further here. A recent study comparing the strengths and weaknesses of several polarization interrogation schemes has been recently published.[25]

For PPOP,[21] the CPT light is modulated between σ_+ and σ_- polarizations with a modulation frequency of ν_{HF} - the frequency of the hyperfine ground-state splitting. For atoms in the dark state, the longitudinal electron spin oscillates at ν_{HF}, and by exciting the atoms in phase with the dark-state coherence, atoms are efficiently pumped out of the end magnetic trap states and into the dark state. The enhancement of the contrast achieved with PPOP over excitation with a single circular polarization depends on the buffer-gas pressure and composition, the light intensity, and the size and temperature of the cell, but enhancement factors of nearly 80× have been observed in buffer-gas vapor cells.[21,26] Equivalently, the lin $\perp$ lin scheme[23] has demonstrated similar contrast improvement[23,27–29] but by using orthogonal linearly polarized light for the two optical frequency components, which are each the sum of σ_+ and σ_- polarizations.

For the $\sigma_+ - \sigma_-$ scheme,[22,30] the double-Λ system is formed with a left (right) circularly polarized input beam and a right (left) circularly polarized counter-propagating beam, which is easily achieved by retroreflecting the CPT light back through a quarter-wave plate and through the atoms a second time. Although $\sigma_+ - \sigma_-$ was demonstrated very soon after PPOP, only one prior experiment using the technique has been published,[30] which reported that the CPT signal amplitude was improved by only a factor of 1.4 over traditional CPT excitation based on a σ_+ travelling wave of the same intensity. However, the observed enhancement was limited by low laser power and not by the technique itself.

a)Author to whom correspondence should be addressed: elizabeth.donley@nist.gov

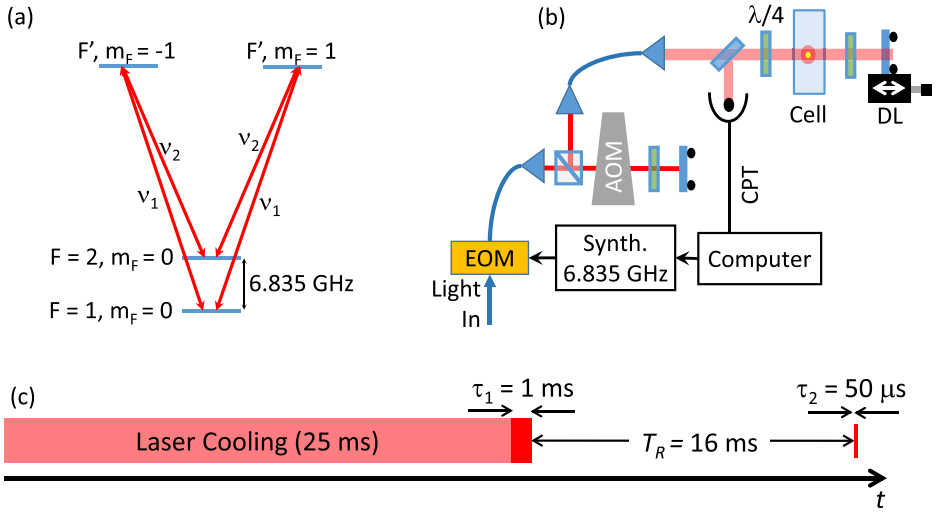

FIG. 1. (a) Double-Λ systems probed with the PPOP, $\sigma_+ - \sigma_-$, and lin⊥lin schemes for ^{87}Rb ($I = 3/2$). The techniques work when the optical frequency is tuned to either the $|F'=1,2\rangle$ state. (b) Simplified diagram of the experimental apparatus. The MOT laser beams are not shown. (c) Timing diagram for an experimental sequence. Single-pulse spectra are extracted from the end of the first pulse, and Ramsey spectra are extracted from the beginning of the second pulse.

In this work, we demonstrate that the $\sigma_+ - \sigma_-$ scheme indeed achieves the same characteristic contrast enhancement as the other equivalent schemes. Similar to recent experiments based on the lin ∥ lin technique,[16] we show that the use of laser-cooled atoms allows for nearly complete dark state formation, which is not typical for atoms in buffer-gas vapor cells in which ground-state relaxation is more significant. We also operate the system as a clock with Ramsey-type interrogation[31] and characterize its frequency stability.

The apparatus has been described previously[16] and is described only briefly here. The atoms are trapped and cooled in a magneto-optical trap (MOT) by a distributed Bragg reflector (DBR) laser frequency-stabilized on the ^{87}Rb D2 line with typically a 25 ms cooling period and 3.5 mW of total cooling light. After the cooling period, the atoms are released and interrogated while in free fall. Typically, the MOT can trap 5×10^6 atoms, and the atoms are recaptured between cycles.[32]

The CPT laser source is a second DBR laser resonant on the ^{87}Rb D1 line at 795 nm and frequency stabilized to the $|F = 1\rangle$ to $|F' = 2(\text{or } 1)\rangle$ optical transition. The interrogation spectrum for CPT is produced by modulating the light with an electro-optic phase modulator (EOM) driven with a 6.835 GHz microwave signal [see Fig. 1(b)]. The carrier and -1st-order sideband interrogate the atoms, with the microwave power set such that the intensities of each of the 1st-order sidebands are equal to the intensity of the carrier. An acousto-optic modulator (AOM) serves as the on/off switch for the light and shifts the optical frequencies that were offset locked in a saturated absorption spectrometer to resonance. The CPT beam is divided into two sub-beams by a beam splitter. Part of the light is sent to a photodiode whose signal normalizes the CPT spectra (not shown). The other beam propagates through a quarter-wave plate before passing through the cold atoms and a second quarter-wave plate before it is retroreflected by a mirror fixed to a translation stage. The beam then passes through the atoms and waveplates a second time before it is detected. The translation stage is adjusted to achieve maximum signal amplitude.[30]

CPT resonances can be measured in both "single-pulse" and "Ramsey" modes [see Fig. 1(c)]. In the single-pulse mode, the light is applied at a fixed modulation frequency in a typical pulse of 1–3 ms duration after the atoms are released from the MOT, and the transmission at the end of the pulse is recorded. The frequency is then changed, and the measurement sequence is repeated to collect the spectrum. In the Ramsey mode, the first CPT pulse pumps the atoms into the dark state, and the transmission is measured during the first 50 μs of the second pulse after a typical Ramsey period of 16 ms, which is optimal given the 3.6 mm CPT beam diameter ($1/e^2$). Typical single-pulse CPT resonances detected with σ_+ polarization in a single travelling wave and a $\sigma_+ - \sigma_-$ counter-propagating standing wave are shown in Fig. 2.

The absorption contrast, which characterizes the completeness of dark-state formation, is defined as the ratio of the depths of the CPT and optical absorption resonances and is approximately 90% for the data shown in red in Fig. 2(b). This high value is achieved because the lifetime of the ground state coherence is limited by background Rb collisions to 75 ms, which is much longer than the CPT pulse length of 3 ms. Since the absorption contrast reflects the completeness of dark state formation, it also relates to the resonant light shift and the long-term clock stability since residual resonant light shifts[33,34] are eliminated when complete dark states are formed, which was recently confirmed for this cold-atom CPT experiment.[16] In contrast, CPT resonances in buffer-gas vapor cells typically exhibit absorption contrasts in the range of 0.1–10%.[4,8,35]

The transmission contrast, defined as the ratio of the resonance transmission to the background (S/B), is typically limited to between 3 and 4% in this cold-atom system because the diameter of the cold-atom cloud is one fourth as large as the CPT beam diameter. The relatively large beam diameter of 3.6 mm ($1/e^2$) is used because the atoms fall by almost 2 mm during a typical interrogation period of 20 ms. The S/B can be much higher in buffer-gas cells, which have higher optical thickness. The S/B more directly affects the clock's stability and is more typically cited. S/B values of over 50% have been observed in buffer-gas cells using PPOP[26] and lin ⊥ lin,[36] and even higher values can be observed with techniques like polarization-selective detection[9] and four-wave mixing.[37]

Figure 3(a) compares the amplitude of the CPT resonance as a function of the total optical intensity for σ_+ and

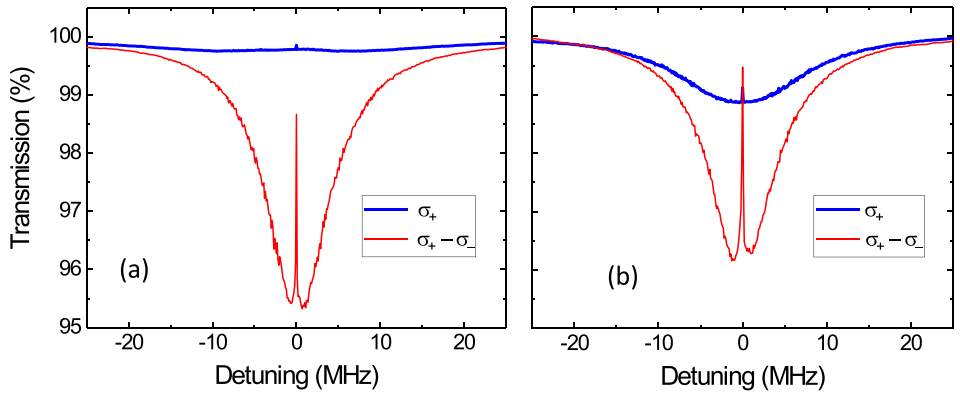

FIG. 2. Cold-atom CPT spectra collected in the single-pulse mode for the σ_+ and $\sigma_+ - \sigma_-$ interrogation schemes versus detuning of the EOM modulation frequency from the accepted value of ν_{HF}. Each data point was measured in one shot with one cold-atom sample. In (a), the total intensity of 0.13 mW/cm^2 was used for both curves. In (b), intensities close to the optimized values for maximum contrast were used for each curve, which were 0.036 mW/cm^2 for σ_+ interrogation and 0.33 mW/cm^2 for $\sigma_+ - \sigma_-$ interrogation. For all data, the duration of the CPT pulse was 3 ms, and the optical frequencies were resonant with the $|F'=1\rangle$ state. For these broad absorption spectra, the frequency step size (100 kHz) is large compared to the power-broadened width of the CPT resonances (typically 10 kHz), but since the resonances are all centered on ν_{HF} to within a 10 Hz, the center point is an accurate measure of the resonant transmission. The CPT and optical resonances are slightly offset from each other because of small offsets of the carrier frequency from the optical resonance.

$\sigma_+ - \sigma_-$ interrogation. The CPT beams for the σ_+ configuration were not retroreflected, but otherwise the experimental conditions were identical. For σ_+ interrogation, the amplitude of the CPT resonance signal initially grows with increasing intensity but reaches a maximum and then decreases with higher intensity. For the $\sigma_+ - \sigma_-$ configuration, the CPT signal grows with higher intensity and levels off above 0.1 mW/cm^2.

In the counter-propagating configuration, complete dark states only form for atoms at positions along the CPT beam where the phases of the CPT coherences created by the forward- and backward-beams add constructively.[22,30] At other positions, the resonances are smaller due to destructive interference. As a result, the CPT amplitude varies as a function of the retroreflecting mirror position as shown in Fig. 3(b) with adjacent maxima separated by half the wavelength of the microwave transition (∼22 mm). Because of this, the $\sigma_+ - \sigma_-$ technique works best for small cells or laser-cooled atoms, where the size of the interrogation region is much smaller than the microwave wavelength. Since the retroreflected geometry also naturally reduces the Doppler shift for laser-cooled atoms,[14] the technique is naturally suited for cold-atom clocks.

A zoomed-in spectrum of a typical CPT resonance corresponding to the red curve in Fig. 2(a) is shown in Fig. 4(a). The two satellite peaks centered at ±62 kHz are the $\Delta m_F = 0$ magnetically sensitive transitions between the $m_F = \pm 1$ magnetic sublevels. The resonances are power broadened to a width of 28(1) kHz, consistent with the expected width[38] for an optical intensity of 0.13 mW/cm^2 with ∼2/3 of the optical power in the resonant sidebands.

Given the signal-to-noise ratio (S/N) and the linewidth, the clock stability that would be supported by these single-pulse resonances can be estimated, but in the example of Fig. 4(a), the stability would not be very good because of the strong power broadening. Most clock measurements done so far with this system have been performed with Ramsey interrogation, which is not affected by power broadening. A typical Ramsey spectrum fitted to a sinusoid is shown in Fig. 4(b). From the resonance width and S/N, one predicts a clock stability of $7 \times 10^{-12}/\sqrt{\tau}$—within a factor of two of the

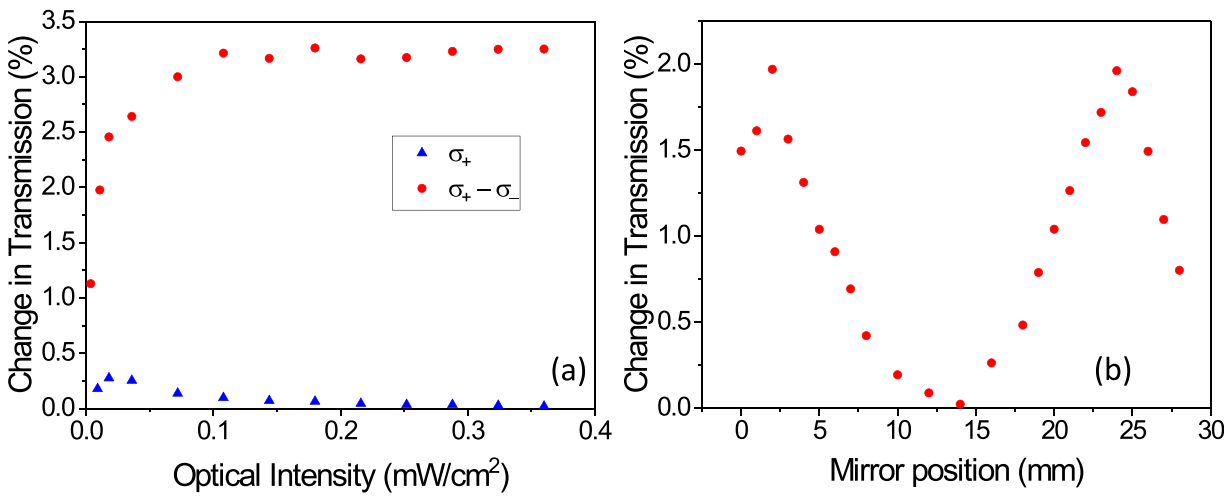

FIG. 3. (a) Amplitude of the CPT resonance versus the total intensity of the CPT light for the $\sigma_+ - \sigma_-$ and σ_+ configurations. The duration of the CPT pulse was 3 ms, and the CPT light was resonant with the $|F'=1\rangle$ excited state. (b) Single-pulse CPT resonance transmission versus the relative mirror position for $\sigma_+ - \sigma_-$ interrogation. The total CPT intensity was 0.18 W/m^2, and the length of the CPT pulse was 3 ms. The CPT light was resonant with the $|F'=2\rangle$ excited state.

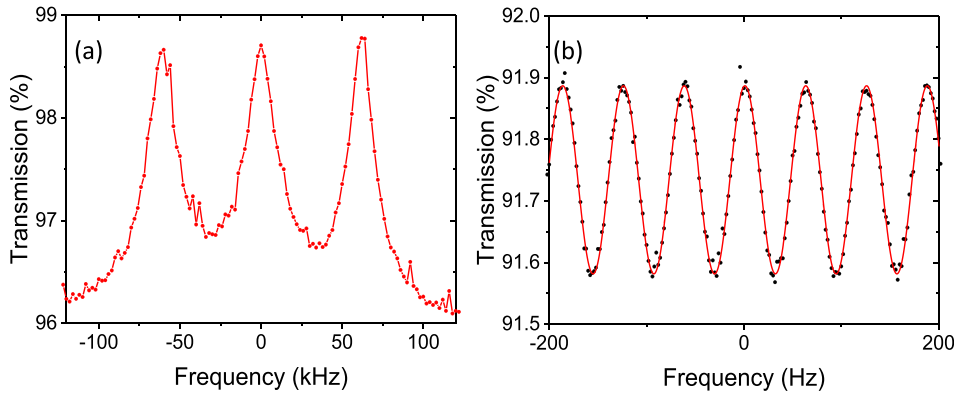

FIG. 4. (a) A typical power-broadened single-pulse spectrum collected with a cycle period of 27.5 ms and a total optical intensity of 0.1 mW/cm^2. The duration of the CPT pulse was 1 ms, and the signal was integrated for the final 500 μs of the pulse. (b.) The central fringes of a typical Ramsey spectrum fitted to a sinusoid. The cycle period was 44 ms. The fitted fringe width of 31.21(2) Hz agrees well with the expected width of 31.25 Hz for a 16 ms Ramsey period. The signal is extracted from the first 50 μs of the second pulse and normalized to the final 200 μs of the first pulse. The single-shot S/N is 44. The position of the central Ramsey fringe agrees with the second-order Zeeman shift of 1.13 Hz. For both spectra, the CPT light was resonant with the $|F'=1\rangle$ excited state.

measured stability plotted in Fig. 5. The clock frequency stability is $1.3 \times 10^{-11}/\sqrt{\tau}$ and reaches 1.8×10^{-13} after 40 000 s. This long-term stability is about a factor of 10 better than what was achieved with an earlier cold-atom CPT system based on phase locking,[14] and this improvement is attributed to the elimination of the resonant transient shift.[15,16] The dominant noise sources that limit the short-term stability with roughly equal contributions are laser intensity noise, laser frequency noise, and microwave phase fluctuations. Persisting long-term instabilities may arise from variations in the relative intensities of the two CPT frequency components[8,39] and residual Doppler shifts,[14] which are topics of continued study. The short-term stability achieved in a recent study using the lin ∥ lin technique was very similar,[16] but here the measurements were performed for an integration period that was six times longer.

It is interesting to compare the clock presented here with the state-of-the-art in thermal cell-based clocks. Vapor-cell Rb clocks based on the double-resonance pulsed optical pumping (POP) technique[40–42] employ laser state selection and detection combined with traditional Ramsey microwave interrogation. POP clocks have achieved outstanding stability, approaching 1×10^{-13} at 1 s and 1×10^{-14} at one day, competitive in long-term stability with the vapor-cell Rb clocks used in the current generation of GPS satellites.[43] This long-term stability is achieved in spite of the cell temperature stability requirement of 100 μK per day arising from the large buffer-gas shift of 4.3 kHz and the cell temperature coefficient of 1×10^{-10}/°C.[40]

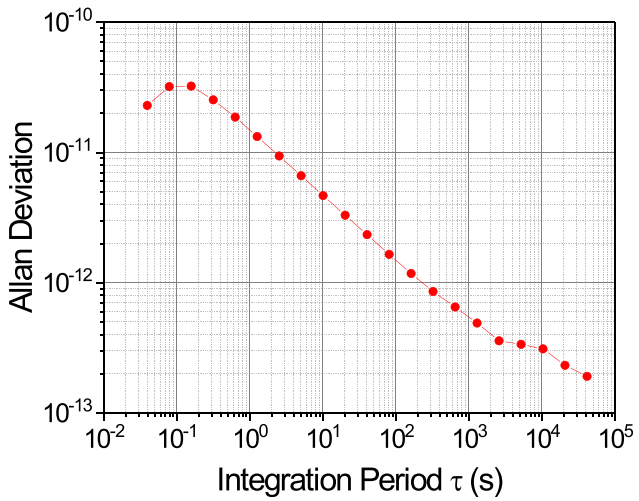

FIG. 5. Frequency stability of cold-atom CPT clock achieved with $\sigma_+ - \sigma_-$ interrogation. The light was resonant with the $|F'=2\rangle$ transition, the length of the first pulse was 1 ms, the length of the second pulse was 50 μs, the intensity was 0.05 mW/cm^2, and the Ramsey period was 16 ms.

The cold-atom CPT clock presented here interrogates many orders of magnitude fewer atoms than POP clocks and its instability is about a factor of 100 worse at 1 s and 25 worse at 40 000 s. But cold-atom CPT clocks may nevertheless lend themselves to applications in the field, given the absence of buffer-gas shifts and resulting low temperature coefficients and their potential for being smaller and lower power.

J. W. Pollock, J. Elgin, C. Oates, and E. Ivanov are gratefully acknowledged for technical help and discussions. V. I. Yudin was supported by the Russian Scientific Foundation (Project No. 16-12-00052), Ministry of Education and Science of the Russian Federation (Project No. 3.1326.2017/4.6), and Russian Foundation for Basic Research (Project No. 17-02-00570). This work is a contribution of NIST, an agency of the U.S. government, and is not subject to copyright.

[1]G. Alzetta, A. Gozzini, L. Moi, and G. Orriols, Il Nuovo Cimento **36**, 5 (1976).
[2]E. Arimondo, Prog. Opt. **35**, 257–354 (1996).
[3]J. Vanier, Appl. Phys. B **81**(4), 421–442 (2005).
[4]V. Shah and J. Kitching, Adv. At., Mol., Opt. Phys. **59**, 21 (2010).
[5]S. Knappe, V. Shah, P. D. D. Schwindt, L. Hollberg, J. Kitching, L.-A. Liew, and J. Moreland, Appl. Phys. Lett. **85**, 1460–1462 (2004).
[6]R. Lutwak, P. Vlitas, M. Varghese, M. Mescher, D. K. Serkland, and G. M. Peake, in *Proceedings of the IEEE International Frequency Control Symposium and Exposition* (2005), pp. 752–757.
[7]R. Lutwak, in *43rd Annual Precise Time and Time Interval Systems and Applications Meeting* (Long Beach, CA, 2011), pp. 207–220.
[8]M. Zhu and L. S. Cutler, in *32th Annual Precise Time and Time Interval Systems and Applications Meeting* (Reston, Virginia, 2000), pp. 311–324.
[9]M. Zhu, in *Proceedings of the IEEE International Frequency Control Symposium and PDA Exhibition Jointly with the 17th European Frequency and Time Forum* (Tampa, FL, 2003), pp. 16–21.
[10]J.-M. Danet, M. Lours, P. Yun, S. Guérandel, and E. D. Clercq, in *Proceedings of the Joint European Frequency and Time Forum and*

International Frequency Control Symposium (Prague, Czech Republic, 2013), pp. 586–589.
[11]M. A. Hafiz, G. Coget, P. Yun, S. Guérandel, E. D. Clercq, and R. Boudot, J. Appl. Phys. **121**(10), 104903 (2017).
[12]P. Yun, F. Tricot, C. E. Calosso, S. Micalizio, B. François, R. Boudot, S. Guérandel, and E. de Clercq, Phys. Rev. Appl. **7**(1), 014018 (2017).
[13]C. Xi, Y. Guo-Qing, W. Jin, and Z. Ming-Sheng, Chin. Phys. Lett. **27**(11), 113201 (2010).
[14]F. X. Esnault, E. Blanshan, E. N. Ivanov, R. E. Scholten, J. Kitching, and E. A. Donley, Phys. Rev. A **88**(4), 042120 (2013).
[15]E. Blanshan, S. M. Rochester, E. A. Donley, and J. Kitching, Phys. Rev. A **91**(4), 041401 (2015).
[16]X. Liu, E. Ivanov, V. I. Yudin, J. Kitching, and E. A. Donley, Phys. Rev. Appl. **8**(5), 054001 (2017).
[17]V. Shah, M. Mescher, A. Martins, J. Leblanc, N. Byrne, B. Timmons, R. Stoner, F. Rogamentich, and R. Lutwak, in *43rd Annual Precise Time and Time Interval (PTTI) Systems and Applications Meeting* (Long Beach, California, 2011), pp. 221–230.
[18]V. Shah, R. Lutwak, R. Stoner, and M. Mescher, in *IEEE International Frequency Control Symposium Proceedings* (2012), pp. 1–6.
[19]J. Sebby-Strabley, K. Salit, K. Nelson, J. Ridley, and J. Kriz, in *Proceedings of the 43rd Annual Precise Time and Time Interval Systems and Applications Meeting* (Long Beach, CA, 2011), pp. 231–238.
[20]J. A. Rushton, M. Aldous, and M. D. Himsworth, Rev. Sci. Instrum. **85**(12), 121501 (2014).
[21]Y. Y. Jau, E. Miron, A. B. Post, N. N. Kuzma, and W. Happer, Phys. Rev. Lett. **93**(16), 160802 (2004).
[22]A. V. Taichenachev, V. I. Yudin, V. L. Velichansky, S. V. Kargapoltsev, R. Wynands, J. Kitching, and L. Hollberg, JETP Lett. **80**(4), 236–240 (2004).
[23]T. Zanon, S. Guerandel, E. de Clercq, D. Holleville, N. Dimarcq, and A. Clairon, Phys. Rev. Lett. **94**(19), 193002 (2005).
[24]A. V. Taichenachev, V. I. Yudin, V. L. Velichansky, and S. A. Zibrov, JETP Lett. **82**(7), 398–403 (2005).
[25]Z. Warren, M. S. Shahriar, R. Tripathi, and G. S. Pati, Metrologia **54**(4), 418 (2017).
[26]X. Liu, J.-M. Merolla, S. Guerandel, C. Gorecki, E. de Clercq, and R. Boudot, Phys. Rev. A **87**, 013416 (2013).
[27]O. Kozlova, J.-M. Danet, S. Guérandel, and E. D. Clercq, IEEE Trans. Instrum. Meas. **63**(7), 1863–1870 (2014).
[28]J.-M. Danet, O. Kozlova, P. Yun, S. Guérandel, and E. de Clercq, EPJ Web Conf. **77**, 00017 (2014).
[29]N. Castagna, S. Guerandel, F. Dahes, T. Zanon, E. d. Clercq, A. Clairon, and N. Dimarcq, in *IEEE International Frequency Control Symposium Joint with the 21st European Frequency and Time Forum* (2007), pp. 67–70.
[30]S. V. Kargapoltsev, J. Kitching, L. Hollberg, A. V. Taichenachev, V. L. Velichansky, and V. I. Yudin, Laser Phys. Lett. **1**(10), 495 (2004).
[31]J. E. Thomas, P. R. Hemmer, S. Ezekiel, C. C. Leiby, R. H. Picard, and C. R. Willis, Phys. Rev. Lett. **48**(13), 867–870 (1982).
[32]H. J. McGuinness, A. V. Rakholia, and G. W. Biedermann, Appl. Phys. Lett. **100**(1), 011106 (2012).
[33]P. R. Hemmer, M. S. Shahriar, V. D. Natoli, and S. Ezekiel, J. Opt. Soc. Am. B **6**(8), 1519–1528 (1989).
[34]M. S. Shahriar, P. R. Hemmer, D. P. Katz, A. Lee, and M. G. Prentiss, Phys. Rev. A **55**(3), 2272–2282 (1997).
[35]R. Lutwak, D. Emmons, W. Riley, and R. M. Garvey, in *34th Annual Precise Time and Time Interval (PTTI) Meeting* (Reston, Virginia, 2002), pp. 539–550.
[36]S. A. Zibrov, V. L. Velichansky, A. S. Zibrov, A. V. Taichenachev, and V. I. Yudin, Opt. Lett. **31**(13), 2060–2062 (2006).
[37]V. Shah, S. Knappe, L. Hollberg, and J. Kitching, Opt. Lett. **32**(10), 1244–1246 (2007).
[38]J. Vanier, M. W. Levine, D. Janssen, and M. J. Delaney, IEEE Trans. Instrum. Meas. **52**(3), 822–831 (2003).
[39]J. Vanier, A. Godone, and F. Levi, in *Proceedings of the 1999 Joint Meeting of the European Frequency and Time Forum and the IEEE International Frequency Control Symposium* (Besancon, 1999), Vol. 1, pp. 96–99.
[40]S. Micalizio, C. E. Calosso, A. Godone, and F. Levi, Metrologia **49**(4), 425 (2012).
[41]S. Micalizio, A. Godone, C. Calosso, F. Levi, C. Affolderbach, and F. Gruet, IEEE Trans. Ultrason., Ferroelectrics, Freq. Control **59**(3), 457–462 (2012).
[42]S. Micalizio, F. Levi, A. Godone, C. E. Calosso, B. François, R. Boudot, C. Affolderbach, S. Kang, M. Gharavipour, F. Gruet, and G. Mileti, J. Phys.: Conf. Ser. **723**(1), 012015 (2016).
[43]R. T. Dupuis, T. J. Lynch, and J. R. Vaccaro, in *IEEE International Frequency Control Symposium* (2008), pp. 655-–660.